Xylose phosphorylation functions as a molecular switch to regulate proteoglycan biosynthesis

Jianzhong Wen[a], Junyu Xiao[a,1], Meghdad Rahdar[a], Biswa P. Choudhury[b], Jixin Cui[a], Gregory S. Taylor[a], Jeffrey D. Esko[b,c], and Jack E. Dixon[a,2]

Departments of [a]Pharmacology and [b]Cellular and Molecular Medicine, and [c]Glycobiology Research and Training Center, University of California, San Diego, La Jolla, CA 92093

Contributed by Jack E. Dixon, September 26, 2014 (sent for review August 22, 2014)

Most eukaryotic cells elaborate several proteoglycans critical for transmitting biochemical signals into and between cells. However, the regulation of proteoglycan biosynthesis is not completely understood. We show that the atypical secretory kinase family with sequence similarity 20, member B (Fam20B) phosphorylates the initiating xylose residue in the proteoglycan tetrasaccharide linkage region, and that this event functions as a molecular switch to regulate subsequent glycosaminoglycan assembly. Proteoglycans from *FAM20B* knockout cells contain a truncated tetrasaccharide linkage region consisting of a disaccharide capped with sialic acid (Siaα2–3Galβ1–4Xylβ1) that cannot be further elongated. We also show that the activity of galactosyl transferase II (GalT-II, B3GalT6), a key enzyme in the biosynthesis of the tetrasaccharide linkage region, is dramatically increased by Fam20B-dependent xylose phosphorylation. Inactivating mutations in the *GALT-II* gene (*B3GALT6*) associated with Ehlers-Danlos syndrome cause proteoglycan maturation defects similar to *FAM20B* deletion. Collectively, our findings suggest that GalT-II function is impaired by loss of Fam20B-dependent xylose phosphorylation and reveal a previously unappreciated mechanism for regulation of proteoglycan biosynthesis.

secretory kinase | proteoglycan | xylose phosphorylation | Fam20B | GalT-II

The human genome encodes more than 500 protein kinases, most of which phosphorylate protein substrates in the nucleus and cytosol and play important roles in cell signaling (1, 2). Kinases that specifically phosphorylate glycans have only rarely been reported and our knowledge of their physiological functions remains in its infancy (3–5). Fam20B (family with sequence similarity 20, member B) is a recently identified atypical secretory pathway kinase (6, 7). Genetic studies have shown that deletion of *Fam20B* in mice results in embryonic lethality at embryonic day 13.5 (E13.5), whereas loss-of-function mutations in the *fam20b* gene in *Danio rerio* cause aberrant cartilage formation and severe skeletal defects that are linked to abnormal proteoglycan (PG) biosynthesis (8, 9).

PGs are a special family of glycoconjugates consisting of one or more glycosaminoglycan (GAG) side chains covalently linked to specific Ser residues within a protein core via a common linkage tetrasaccharide [glucuronic acid-β1–3-galactose-β1–3-galactose-β1–4-xylose-β1 (GlcAβ1–3Galβ1–3Galβ1–4Xylβ1)] as illustrated in Fig. 1*A* (10). Mature GAGs are sulfated linear polysaccharides that are further classified as heparan sulfate (HS) or chondroitin/dermatan sulfate (CS), depending on the specific composition of elongated sugar repeats (11). PGs are expressed on the cell surface and in the extracellular matrix of all animal cells and tissues, playing critical roles in cell–cell and cell–matrix interactions and signaling, largely through the attached GAGs (12). The cellular machinery required for PG biosynthesis is conserved over a wide range of eukaryotic organisms and altered PG biosynthesis is associated with numerous human disease states (13–17). Thus, understanding how this process is regulated will be important. Loss of Fam20B appears to decrease the amount of cellular GAG chains and causes profound defects in embryonic development and skeletal formation (6, 8, 9). Fam20B has been reported to have xylose kinase activity against α-thrombomodulin, a glycoprotein bearing the tetrasaccharide linkage fragment. However, the specific molecular mechanism by which Fam20B-dependent xylose phosphorylation regulates PG synthesis is not clear.

Here we provide evidence that Fam20B is a xylose kinase that phosphorylates the initiator xylose residue within the tetrasaccharide linkage region of a wide array of O-linked PGs. We show that Fam20B requires a minimal Gal-Xyl disaccharide motif for activity, and loss of Fam20B-dependent xylose phosphorylation results in premature termination of the tetrasaccharide linkage and impaired glycosaminoglycan assembly. Our findings suggest that phosphorylation of xylose within the linkage region by Fam20B dramatically increases the activity of galactosyltransferase II (GalT-II), an enzyme necessary for completion of the linkage region and efficient glycosaminoglycan assembly. Cells lacking either Fam20B or GalT-II are unable to complete the assembly of the linkage region and exhibit only short sugar stubs within their proteoglycans. Our findings reveal a previously unappreciated mechanism for regulation of proteoglycan assembly and offer insight into the molecular basis of diseases associated with aberrant proteoglycan maturation.

Significance

Proteoglycans are cellular proteins modified with long chains of repeating sugar residues connected to serine residues within the protein core by a short tetrasaccharide linker. Proteoglycans perform critical cellular functions such as formation of the extracellular matrix, binding to a diverse array of molecules, and regulation of cell motility, adhesion, and cell–cell communication. We show here that family with sequence similarity 20, member B (Fam20B) is a xylose kinase that phosphorylates a xylose sugar residue within the proteoglycan tetrasaccharide linkage. Xylose phosphorylation dramatically stimulates the activity of galactosyltransferase II (GalT-II, B3GalT6), an enzyme that adds galactose to the growing linkage. Cells lacking Fam20B cannot extend the tetrasaccharide linkage and thus have immature and nonfunctional proteoglycan, a phenotype remarkably similar to Ehlers-Danlos syndrome caused by inactivating GalT-II mutations.

Author contributions: J.W., J.X., M.R., G.S.T., J.D.E., and J.E.D. designed research; J.W., J.X., M.R., B.P.C., J.C., and G.S.T. performed research; J.D.E. contributed new reagents/analytic tools; J.W., J.X., M.R., B.P.C., J.C., G.S.T., J.D.E., and J.E.D. analyzed data; and J.W., G.S.T., and J.E.D. wrote the paper.

The authors declare no conflict of interest.

Freely available online through the PNAS open access option.

[1]Present address: State Key Laboratory of Protein and Plant Gene Research, School of Life Sciences, and Peking-Tsinghua Center for Life Sciences, Peking University, Beijing 100871, China.

[2]To whom correspondence should be addressed. Email: jedixon@ucsd.edu.

This article contains supporting information online at www.pnas.org/lookup/suppl/doi:10.1073/pnas.1417993111/-/DCSupplemental.

Results and Discussion

Fam20B Is a Proteoglycan Xylose Kinase. Fam20B belongs to a recently identified family of secretory pathway kinases that includes Fam20C, which phosphorylates secretory proteins within a highly conserved Ser-X-Glu/pSer motif (7, 18). Although Fam20B shares nearly 60% sequence similarity with Fam20C, it does not phosphorylate proteins; rather, Fam20B has been reported to phosphorylate the xylose residue within the tetrasaccharide linkage of α-thrombomodulin (6, 19). To test whether authentic PGs could serve as substrates for Fam20B, we took advantage of the fact that xylose phosphorylation on mature PGs has been reported to be substoichiometric (20). We therefore immunopurified FLAG-tagged decorin from conditioned medium of HEK293T cells and performed an in vitro kinase reaction with recombinant Fam20B in the presence of [γ-^{32}P]ATP (21). Fam20B indeed efficiently phosphorylated DCN in a time-dependent manner, whereas mutation of the conserved metal binding Asp to Ala (D309A, Fam20B-D/A) abolished its kinase activity (Fig. 1 *B* and *C*). Glycosylated DCN migrated as an elongated smear during gel electrophoresis due to the heterogeneity of attached GAGs. However, treatment with chondroitinase ABC (Chon-ABC), a lyase that specifically digests CS chains but leaves the linkage tetrasaccharide with a single attached disaccharide intact (22), effectively converted DCN into a homogeneous species without affecting ^{32}P signal strength. Moreover, a purified DCN mutant protein (DCN-S34A) that lacked the single GAG attachment site was unable to serve as a substrate for Fam20B (Fig. S1). Thus, Fam20B phosphorylated DCN within the linkage tetrasaccharide in vitro. Fam20B also exhibited kinase activity toward other PGs in the linkage tetrasaccharide, such as cell surface syndecans (SDC1 and SDC4) and cartilage matrix aggrecan (Fig. S2). We next depleted Fam20B in MRC-5 lung fibroblast cells using lentiviral-based short hairpin RNAs and metabolically labeled the cells with [^{32}P]orthophosphate. Endogenous DCN immunoprecipitated from Fam20B knockdown cells contained a significantly decreased amount of ^{32}P compared with DCN imunoprecipitated from control cells (Fig. 1*D*). Together, these data demonstrate that Fam20B phosphorylates PGs within the linkage tetrasaccharide in vitro and in cells.

To further characterize Fam20B kinase activity, we synthesized the linkage tetrasaccharide with a benzyl group at the reducing end (hereafter referred to as "Tetra-Ben") as a model substrate to monitor Fam20B activity (Fig. 1*E*). Fam20B effectively

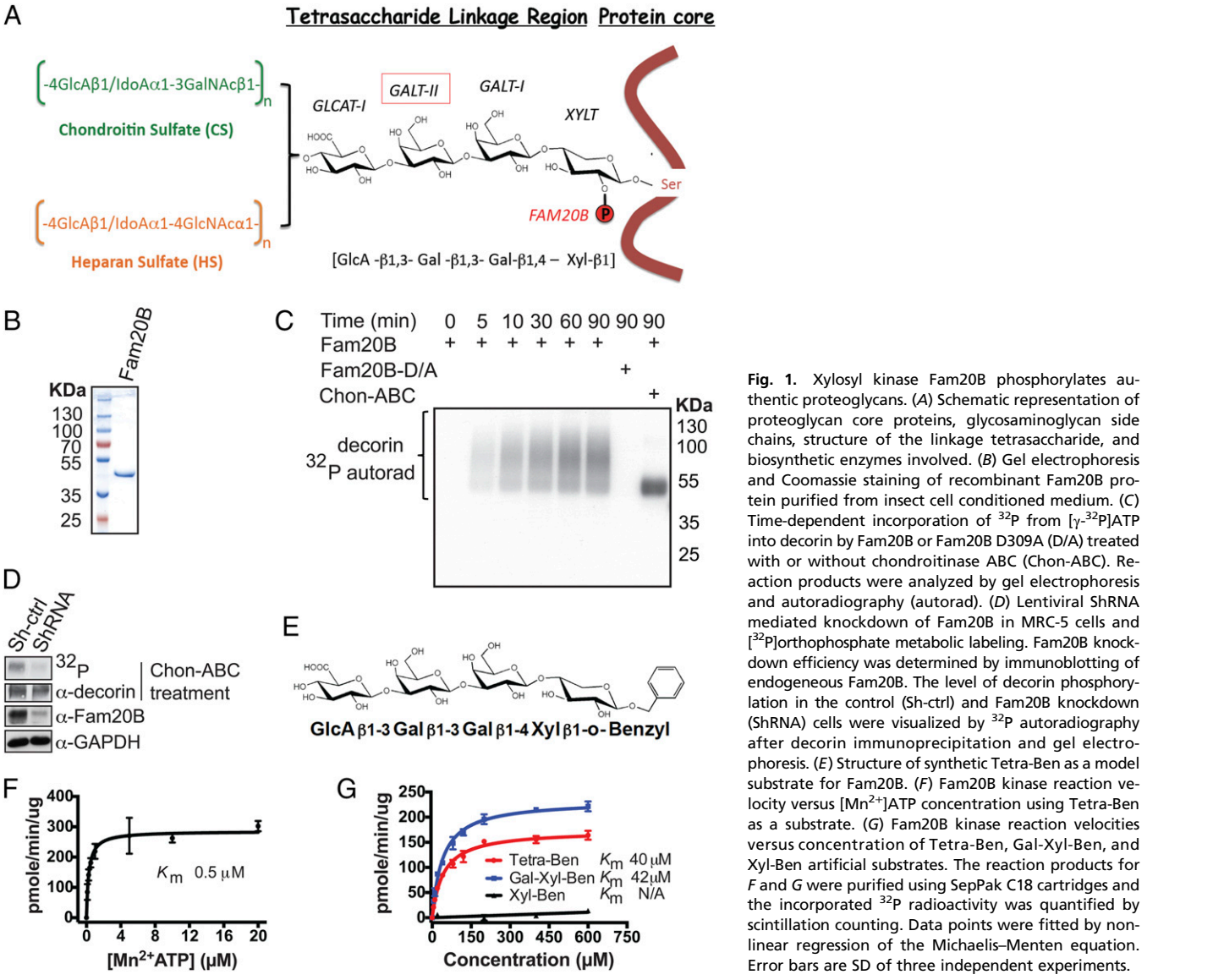

Fig. 1. Xylosyl kinase Fam20B phosphorylates authentic proteoglycans. (*A*) Schematic representation of proteoglycan core proteins, glycosaminoglycan side chains, structure of the linkage tetrasaccharide, and biosynthetic enzymes involved. (*B*) Gel electrophoresis and Coomassie staining of recombinant Fam20B protein purified from insect cell conditioned medium. (*C*) Time-dependent incorporation of ^{32}P from [γ-^{32}P]ATP into decorin by Fam20B or Fam20B D309A (D/A) treated with or without chondroitinase ABC (Chon-ABC). Reaction products were analyzed by gel electrophoresis and autoradiography (autorad). (*D*) Lentiviral ShRNA mediated knockdown of Fam20B in MRC-5 cells and [^{32}P]orthophosphate metabolic labeling. Fam20B knockdown efficiency was determined by immunoblotting of endogeneous Fam20B. The level of decorin phosphorylation in the control (Sh-ctrl) and Fam20B knockdown (ShRNA) cells were visualized by ^{32}P autoradiography after decorin immunoprecipitation and gel electrophoresis. (*E*) Structure of synthetic Tetra-Ben as a model substrate for Fam20B. (*F*) Fam20B kinase reaction velocity versus [Mn^{2+}]ATP concentration using Tetra-Ben as a substrate. (*G*) Fam20B kinase reaction velocities versus concentration of Tetra-Ben, Gal-Xyl-Ben, and Xyl-Ben artificial substrates. The reaction products for *F* and *G* were purified using SepPak C18 cartridges and the incorporated ^{32}P radioactivity was quantified by scintillation counting. Data points were fitted by nonlinear regression of the Michaelis–Menten equation. Error bars are SD of three independent experiments.

phosphorylated Tetra-Ben in a time-dependent manner in vitro (Fig. S3 *A* and *B*). Mass spectrometry (MS) analysis of the reaction products confirmed phosphorylation of xylose within this artificial substrate (Fig. S3 *C* and *D*). Using the Tetra-Ben substrate, we further characterized the enzymatic properties of Fam20B and determined it had a K_m for ATP of 0.5 μM and a K_m of 40 μM for Tetra-Ben (Fig. 1 *F* and *G*). Importantly, Fam20B xylose kinase activity required a minimal disaccharide motif, as Fam20B could phosphorylate Galβ1–4Xylβ1-Ben (V_{max}/K_m = 0.29) as efficiently as Tetra-Ben (V_{max}/K_m = 0.21); however, it was unable to phosphorylate Xylβ1-Ben (Fig. 1*G*). Therefore, Fam20B phosphorylates xylose within the PG linkage tetrasaccharide and has a minimal requirement of a disaccharide for activity.

Xylose-containing glycans are not common in mammalian cells. However, Xyl-Xyl-Glc has been found on EGF-like repeats of the Notch receptor and on other secreted proteins such as the coagulation factors VII, IX, and thrombospondin. The reported structure of this modification is Xylα1–3Xylα1–3Glc (23–25). Fam20B did not exhibit detectable kinase activity against this trisaccharide, further suggesting a strong preference for xylose within the tetrasaccharide linkage.

Fam20B-Dependent Xylose Phosphorylation Is Required for GAG Elongation. To examine the consequence of Fam20B-dependent xylose phosphorylation on PG biosynthesis, we generated *FAM20B* knockout (KO) U2OS (bone osteosarcoma) cells using transcription activator-like effector nuclease (TALEN) targeted to exon 2 of *FAM20B* (Fig. S4). We used these cells to assess the effect of *FAM20B* deletion on cell surface and secreted HS in conjunction with a well-characterized antibody (3G10), which specifically recognizes HS sugar stubs that remain on HSPG core proteins following heparin lyase (hepase) digestion of the HS chains (22, 26). As expected, we detected a number of different PG core proteins that contained the sugar stub neo-epitope upon lyase treatment of WT cells (Fig. 2*A* and Fig. S5 *A* and *B*). However, there was an estimated 95% decrease of overall 3G10 signal in samples derived from *FAM20B* KO cells, indicating a dramatic decrease of global proteoglycan lyase-digestible HS chains (Fig. 2*A*). Further analysis using [^{35}S]sulfate metabolic labeling confirmed the decrease of both HS and CS GAG chains present on the cell surface and in the conditioned medium of *FAM20B* KO cells (Fig. S5*C*).

We hypothesized that the global loss of GAGs we observed in *FAM20B* KO cells was potentially due to altered PG trafficking/secretion, impaired GAG elongation, or both effects simultaneously. When we probed the same 3G10 blot with PG core protein antibodies such as anti-SDC1, we observed that SDC1 from the *FAM20B* WT cells could be detected as a homogeneous band only after lyase treatment (Fig. 2*A*), consistent with the fact that most PGs run as smears and can only be detected as discrete bands by immunoblotting after removing the heterogeneous GAG chains. In contrast, the SDC1 core protein from *FAM20B* KO cells was detectable with similar intensity with or without lyase treatment (Fig. 2*A*). A similar effect was observed for another PG, glypican 1 (GPC1), which was present both on cell surface and in the conditioned medium (Fig. 2*A* and Fig. S5*B*). This gel-based assay suggests that *FAM20B* deletion impairs GAG chain elongation at an early step.

To examine whether trafficking/secretion of PGs with the aberrant sugar stubs was affected in *FAM20B* KO cells, we quantified cell surface SDC1 in *FAM20B* WT and KO cells by flow cytometry. Both WT and KO cells displayed a similar amount of SDC1 on the surface (Fig. 2*B*). Moreover, when intact WT and KO cells were treated with trypsin, SDC1 from the KO cells showed comparable sensitivity to trypsin treatment as in the WT cells (Fig. 2*C*), indicating SDC1 surface display was unaffected by *FAM20B* deletion. Examination of other cell surface or secreted

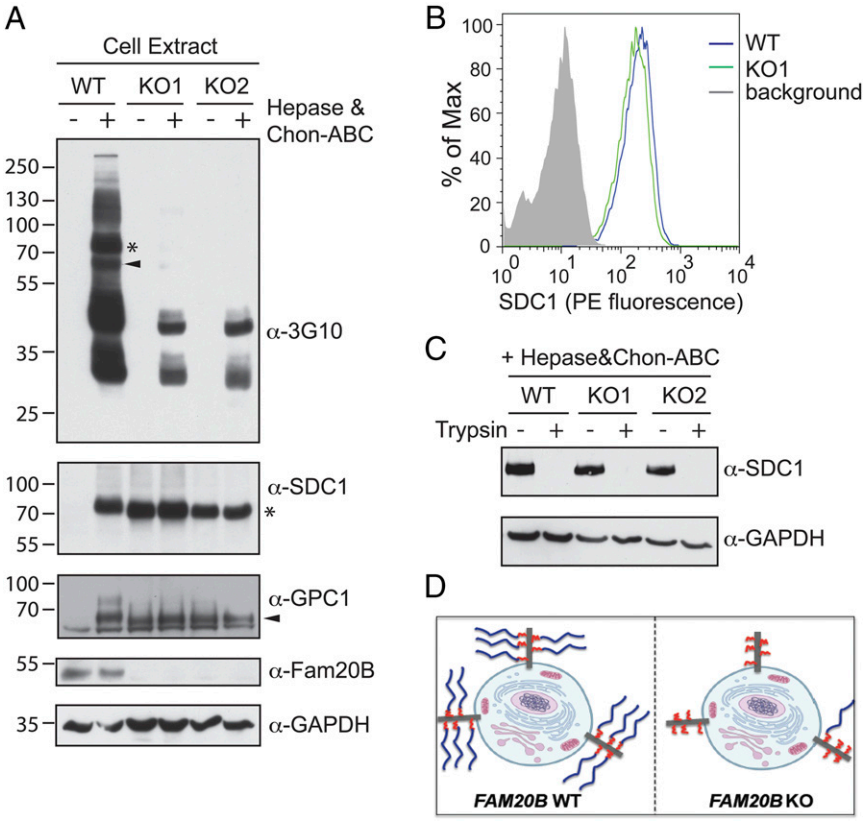

Fig. 2. Xylosyl kinase Fam20B globally regulates glycosaminoglycan chain elongation. (*A*, *Top*) A 3G10 immunoblot of U2OS cell surface proteoglycan heparan sulfate GAG chains from *FAM20B* wild type (WT) and two different *FAM20B* TALEN knockout (KO) clones, with or without heparin lyase (hepase) and Chon-ABC treatment. (*Middle* two panels) Immunoblots of endogeneous Syndecan 1 (SDC1) and Glypican 1 (GPC1) from *FAM20B* WT and KO cells, with or without hepase and Chon-ABC treatment. (*Bottom* two panels) Knockout of *FAM20B* was demonstrated by DNA sequencing and anti-Fam20B immunoblotting, and GAPDH served as a loading control. The electrophoretic mobilities of SDC1 and GPC1 on the 3G10 blot are marked by an asterisk and arrowhead, respectively. (*B*) Quantification of cell surface SDC1 was carried out in the WT and KO cells using flow cytometry with primary anti-SDC1 antibody and PE-labeled secondary antibody. The binding of secondary antibody alone to the cell surface served as a background control measurement. (*C*) Immunoblotting of SDC1 was carried out in intact *FAM20B* WT and KO cells following treatment with or without trypsin. (*D*) Schematic representation of Fam20B function on proteoglycan biosynthesis and sorting. Blue lines represent mature GAG chains and red lines represent short sugar stubs that remain on the core protein in *FAM20B* KO cells.

BIOCHEMISTRY

PGs by flow cytometry also indicated normal trafficking/secretion (Fig. S6). Therefore, we concluded that altered glycosylation caused by *FAM20B* KO did not have a dramatic effect on PG trafficking/secretion (Fig. 2*D*).

We next ectopically expressed DCN and GPC1 in both *FAM20B* WT and KO cells, and immunopurified them from the conditioned medium. We examined GAG elongation of the immunoprecipitated proteins by gel electrophoresis after they were radiolableled by in vitro Fam20B phosphorylation in the presence of [γ-^{32}P]ATP. As expected, the proteins expressed in the WT cells migrated as an elongated smear (Fig. 3*A*). However, ~70% of DCN and more than 90% of GPC1 expressed in the KO cell migrated as a sharp band, suggesting they did not contain elongated GAGs, which further confirmed that *FAM20B* deletion impaired GAG elongation (Fig. 3*A*).

***FAM20B* Deletion Causes the Formation of Siaα2–3Galβ1–4Xylβ1 on GAG Attachment Sites.** To determine the composition of linkage saccharides accumulated on PGs derived from *FAM20B* WT and KO cells, we released O-linked glycans of GPC1 by reductive β-elimination, then permethylated the oligosaccharides and analyzed them by MS (27). We detected a major glycan species with m/z = 810 from GPC1 produced by *FAM20B* KO cells (Fig. 3*B*, *Top*). When we analyzed GPC1 glycans from *FAM20B* KO cells following in vitro phosphorylation by recombinant Fam20B, the m/z = 810 ion quantitatively shifted to m/z = 904 (consistent with the addition of permethylated phosphate) (Fig. 3*B*, *Middle*). Notably, the m/z = 810 ion species was absent in GPC1 glycans released from the WT cells (Fig. 3*B*, *Bottom*). Moreover, the m/z = 810 ion was the dominant species in DCN glycans released from KO cells, and this species was completely absent when a DCN-S34A mutant that lacked the GAG attachment site was analyzed (Fig. S7). Together, these data indicate that m/z = 810 ion species corresponds to the aberrant sugar stub present on PGs derived from *FAM20B* KO cells. The molecular weight of this ion matches permethylated sialic acid (Sia)-galactose-xylitol as a sodium adduct. We further confirmed this identification by sequential multilevel ion fragmentation using collision-induced dissociation (Fig. 3*C*). To define the specific glycosidic linkage, we hydrolyzed the glycans into monosaccharides, followed by reduction with sodium borodeuteride and acetylation to form partially methylated alditol acetate (PMAA) (28). The PMAA sample was then analyzed by gas chromatography (GC)-MS/MS. We detected the signature fragment ion combination (m/z = 161, m/z = 234) of C3-linked galactose (Fig. 3*D*) and the fragment ion combination (m/z = 161, m/z = 205) of C4-linked xylitol (Fig. S8 *C* and *D*). Thus, the assignment of fragment ions in combination with the well-defined early steps of GAG biosynthesis indicate this unique glycan is Siaα2–3Galβ1–4Xylβ1.

Fam20B-Dependent Xylose Phosphorylation Stimulates Synthesis of the Tetrasaccharide Linkage via GalT-II. We did not observe restoration of GAG elongation after treating KO cells with 3F$_{ax}$-peracetyl *N*-acetylneuraminic acid, a general sialyltransferase inhibitor, suggesting that activation of sialyltransferases due to loss of Fam20B-dependent xylose phosphorylation was not the primary cause of impaired GAG elongation (Fig. S9) (29). Based on this observation and the defined composition of the sugar stubs, we hypothesized that xylose phosphorylation by Fam20B might modulate the activity of GalT-II, which transfers the second galactose unit to Gal-Xyl within the linkage tetrasaccharide (30). To determine whether Fam20B-dependent xylose phosphorylation could affect GalT-II activity, we expressed and purified a GalT-II fusion protein that contained an N-terminal maltose binding protein (MBP) using an insect cell expression system. We then tested its in vitro galactosyltransferase activity against unphosphorylated and Fam20B-phosphorylated Gal-Xyl-Ben substrates in the presence of UDP-[6-^{3}H]Gal. Recombinant MBP-GalT-II exhibited a dramatic increase in galactosyltransferase activity toward Gal-Xyl(P)-Ben phosphorylated by Fam20B

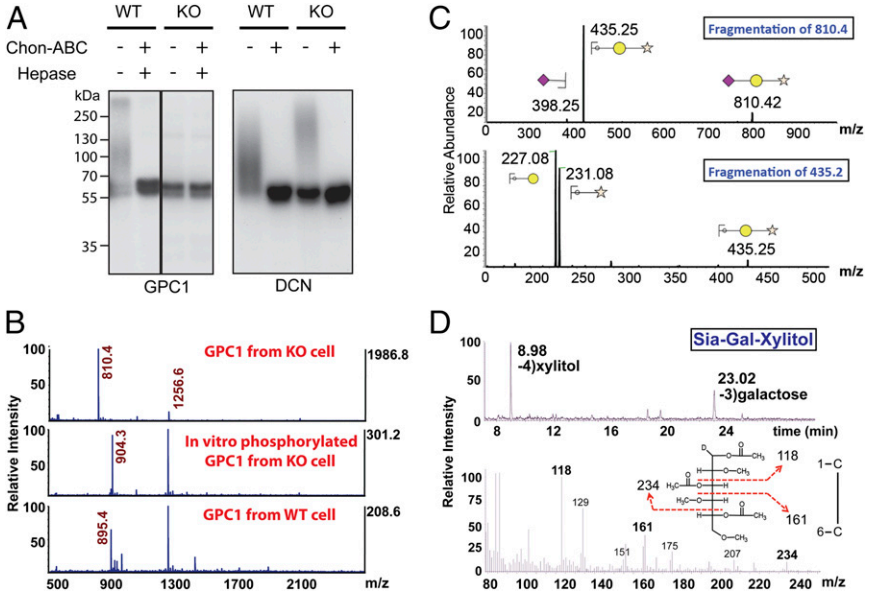

Fig. 3. Identification of Siaα2–3Galβ1–4Xylβ1 on GAG attachment sites on proteoglycans from *FAM20B* deletion cells. (*A*) GPC1 and DCN were purified from *FAM20B* WT and KO cells. An aliquot of purified GPC1 and DCN was phosphorylated using recombinant Fam20B in the presence of [γ-^{32}P]ATP, and each of the samples was then treated with or without Chon-ABC and hepase. The products were separated by gel electrophoresis and incorporated radioactivity was detected by autoradiograph. (*B*, *Top*) The MS analysis of permethylated O-linked glycans released from GPC1 purified from *FAM20B* KO cells (unphosphorylated). (*Middle*) The MS analysis of *FAM20B* KO GPC1 glycans that were phosphorylated by Fam20B in vitro. (*Bottom*) MS analysis for that derived from *FAM20B* WT cells. Note: m/z = 1256.6 was identified as a branched O-glycan (Fig. S8 *A* and *B*). (*C*) Sequential fragmentation of m/z = 810.4 and m/z = 435.2 ion species and the assignment of the fragments. (*D*, *Top*) Gas chromatography profile of alditol acetates derived from hydrolyzed Sia-Gal-Xylitol and the identification of xylitol and galactose retention peaks. (*Bottom*) Fragmentation of galactose (retention time: 23.02 min) and the identification of signature fragment ions of C3 linked Gal (m/z = 118, 161, and 234).

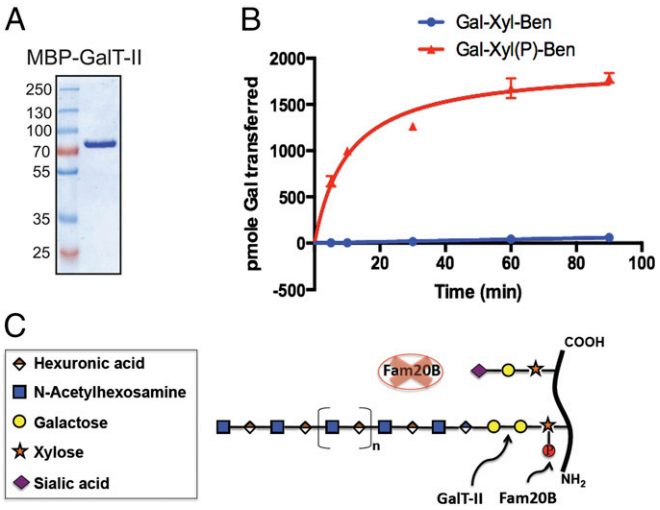

Fig. 4. Fam20B-dependent Xyl phosphorylation markedly stimulates GalT-II activity. (*A*) Gel electrophoresis analysis of recombinant MBP–GalT-II purified from insect cell conditioned medium. (*B*) The relative time-dependent addition of Gal onto Gal-Xyl-Ben and Gal-Xyl(P)-Ben by GalT-II in the presence of UDP-[6-^{3}H]Gal. (*C*) Schematic model depicting the function of Fam20B in GAG biosynthesis.

compared with unphosphorylated Gal-Xyl-Ben (Fig. 4*B*). In the absence of xylose phosphorylation, GalT-II activity toward Gal-Xyl-Ben was decreased to less than 1% of its activity toward phosphorylated Gal-Xyl(P)-Ben. This dramatic decrease in GalT-II activity was consistent with our observations that *FAM20B* deletion in cells caused truncated linkers and dramatically decreased the amount of GAG chains. Moreover, the extremely low residual activity of GalT-II toward unphosphorylated Gal-Xyl-Ben in vitro suggests that it may support a very low level of linkage tetrasaccharide synthesis in cells, providing a plausible explanation why *FAM20B* KO did not completely abrogate GAG elongation. We also determined the kinetic parameters of recombinant MBP-GalT-II toward unphosphorylated Gal-Xyl-Ben and Gal-Xyl(P)-Ben phosphorlyated by Fam20B. The K_m of GalT-II toward Gal-Xyl-Ben was decreased by ∼230-fold after the substrate was phosphorylated on xylose by Fam20B (Fig. S10). These data are consistent with the dramatic increase we observed in the activity of GalT-II against phosphorylated Gal-Xyl(P)-Ben and suggest that xylose phosphorylation stimulates GalT-II turnover primarily by reducing its Michaelis constant. Collectively, these data demonstrate a key mechanism by which Fam20B-dependent xylose phosphorylation within the PG linkage tetrasaccharide stimulates GalT-II activity, allowing successful completion of the linkage fragment and subsequent elongation of GAG chains (Fig. 4*C*). The phosphoxylose may also affect the in vitro activities of other downstream glycosyltransferases in GAG synthesis, but our results indicate its dominant effect is modulating GalT-II activity (31, 32).

Prior studies have shown that the extent of xylose phosphorylation in mature GAGs occurs substoichiometrically. For instance, it was reported that ∼25–50% of GAG chains from SDC1 produced by mouse mammary gland epithelial cells carry xylose phosphorylation, and more than 90% of GAG chains from fly S2 cells have xylose phosphorylation (33, 34). Whether this substoichiometry of phosphorylation arises from incomplete phosphorylation or dephosphorylation is unknown. Some evidence also suggests that xylose phosphorylation of DCN occurs transiently, gradually increasing as the tetrasaccharide linkage is elongated from Gal-Xyl to Gal-Gal-Xyl, then declining via rapid dephosphorylation after the addition of GlcA, indicating the presence of a Golgi phosphatase (20). To that end, Kitagawa and coworkers recently reported a phosphatase with in vitro activity toward phospho-Xyl (35). The timing of xylose phosphorylation during assembly of the tetrasaccharide linkage is likely to be critical. Addition of the second Gal residue to the linkage by GalT-II falls within the time frame of increased xylose phosphorylation and up-regulation of its activity by Fam20B-dependent xylose phosphorylation is fully consistent with the observed transient nature of this event.

Disrupted GAG biosynthesis has been linked to a variety of human pathophysiological conditions (13–17, 36, 37). Inactivating mutations in human *GALT-II* were recently shown to cause Ehlers-Danlos–like syndrome, which is characterized by a spectrum of skeletal and connective tissue disorders (16, 38). Genetic screens in zebrafish have established that *FAM20B* is essential for proper development of cartilage and bone (8). Glycanation of DCN is dramatically decreased in fibroblast cells from *GALT-II* patients (16), similar to DCN derived from *FAM20B* KO cells (Fig. 3*A*). Our results suggest that loss of Fam20B-dependent xylose phosphorylation leads to impaired GalT-II activity, thereby resulting in incomplete linkage tetrasaccharides that are capped with sialic acid and cannot be elongated.

Materials and Methods

Cloning. cDNAs encoding full-length decorin (DCN), glypican 1 (GPC1), and galactosyltransferase II (GalT-II, *B3GALT6*) were purchased from DNASU. Syndecan 1 (SDC1) and syndecan 4 (SDC4) cDNAs were gifts from Gregory Taylor, Department of Pharmacology, University of California, San Diego. The human pCCF-Fam20B construct was generated as described (7). DCN, GPC1, SDC1, and SDC4 ORFs were subcloned into pCCF, and a modified pDisplay expression plasmid encoding a C-terminal strep-tag (a gift from Marnie L. Fusco, The Scripps Research Institute, San Diego) (20, 39–42). Mutagenesis was performed using the Quick-Change Mutagenesis kit (Stratagene). The Fam20B insert from the pCCF vector was also subcloned into the pQCXIP retroviral vector for generating stable cell lines. GalT-II and Fam20B ORFs were subcloned into a modified pSMBP baculovirus vector for protein production (19).

Design of FAM20B TALEN Constructs and Generation of FAM20B Knockout U2OS Cells. To generate *FAM20B* knockout cell lines, a TALEN binding pair was chosen from exon 2 of human *FAM20B*. The genomic recognition sequences used for TALEN left and right arms were: TCAACATGAAGCTAAAGCA (L) and AGCAATTCTCCTTGTCA (R), spaced by 15 bp and anchored by a preceding T base at the −1 position to meet the optimal criteria for natural TAL proteins (43). TALEN vectors containing left and right arms were assembled using the Golden Gate method with HD, NI, NG, and NN modules (repeat-variable di-residue, single letter amino acid code) (44). The cutting efficiency of the designed TALEN was evaluated by the Surveyor assay (45). The resulting left and right TALEN plasmids were cotransfected with pNEGF into U2OS cells by electroporation (Amaxa). After 2 d, cells were sorted using a BD FACSJazz cell sorter in 96-well plate format. *FAM20B* knockout cell clones were screened by PCR and DNA sequencing after 2 wk. Isolated *FAM20B* knockout clones were validated by PCR and DNA sequencing. The absence of Fam20B expression in the selected clones was also confirmed by Fam20B immunoblotting.

Chemical Release of O-Linked Glycans, Permethylation, and MS Analysis. Reductive beta elimination reactions were performed to release O-glycans from 50 μg of proteoglycan samples (46). Briefly, the samples were treated with 50 mM NaOH in the presence of 1 M $NaBH_4$ at 45 °C for 16 h with constant stirring. The samples were cooled in an ice-water bath, neutralized with ice-cold 30% acetic acid, and desalted using cation-exchange resin (Dowex-50W; BioRad). After lyophilization, the dried samples were washed and evaporated three times in a Speed Vac with acidified methanol (MeOH: AcOH 9:1 vol/vol mixture) and MeOH to remove the borate. The samples were then dissolved in H_2O and passed over a Sep-Pak C_{18} cartridge (Waters) to remove proteinaceous components. The purified glycans were permethylated using a modified Ciucanu and Kereks method (47). Briefly, lyophilized O-glycans were dissolved in anhydrous DMSO followed by addition of a NaOH slurry in DMSO and methyliodide (Sigma). After vigorous stirring for 45 min, the reaction was quenched with ice-cold water. The permethylated glycans were extracted using chloroform-water partitioning. The chloroform layers containing the permethylated glycans were dried under nitrogen. The

permethylated glycans were mixed with super-DHB matrix (Sigma) and analyzed by MALDI-TOF (AB SCIEX). Plausible *N*- and O-glycan structures were searched and annotated via the Consortium for Functional Glycomics (CFG) database in GlycoWorkbench software version 1.2.4105 (48). Isolation and fragmentation of parent ions by collision-induced dissociation were performed on an LTQ Orbitrap mass spectrometer (Thermo Scientific). Additional experimental procedures are described in *SI Materials and Methods*.

ACKNOWLEDGMENTS. This work was supported in part by grants from the National Institutes of Health DK018849 and DK018024 (to J.E.D.) and GM33063 and GM93131 (to J.D.E.). We thank Drs. Carolyn Worby and Philip L. Gordts for critically reading the manuscript and members of the J.E.D. laboratory and J.D.E. laboratory for insightful discussions. We thank Dr. Roger Lawrence for technical support with analyzing phospho-Tetra-Ben by mass spectrometry, which was done through the Glycotechnology Core in the Glycobiology Research and Training Center (University of California, San Diego).

1. Manning G, Whyte DB, Martinez R, Hunter T, Sudarsanam S (2002) The protein kinase complement of the human genome. *Science* 298(5600):1912–1934.
2. Cohen P (2002) The origins of protein phosphorylation. *Nat Cell Biol* 4(5):E127–E130.
3. Breloy I, et al. (2012) O-linked N,N′-diacetyllactosamine (LacdiNAc)-modified glycans in extracellular matrix glycoproteins are specifically phosphorylated at subterminal N-acetylglucosamine. *J Biol Chem* 287(22):18275–18286.
4. Fransson LA, Silverberg I, Carlstedt I (1985) Structure of the heparan sulfate-protein linkage region. Demonstration of the sequence galactosyl-galactosyl-xylose-2-phosphate. *J Biol Chem* 260(27):14722–14726.
5. Yoshida-Moriguchi T, et al. (2013) SGK196 is a glycosylation-specific O-mannose kinase required for dystroglycan function. *Science* 341(6148):896–899.
6. Koike T, Izumikawa T, Tamura J, Kitagawa H (2009) FAM20B is a kinase that phosphorylates xylose in the glycosaminoglycan-protein linkage region. *Biochem J* 421(2): 157–162.
7. Tagliabracci VS, et al. (2012) Secreted kinase phosphorylates extracellular proteins that regulate biomineralization. *Science* 336(6085):1150–1153.
8. Eames BF, et al. (2011) Mutations in fam20b and xylt1 reveal that cartilage matrix controls timing of endochondral ossification by inhibiting chondrocyte maturation. *PLoS Genet* 7(8):e1002246.
9. Vogel P, et al. (2012) Amelogenesis imperfecta and other biomineralization defects in Fam20a and Fam20c null mice. *Vet Pathol* 49(6):998–1017.
10. Prydz K, Dalen KT (2000) Synthesis and sorting of proteoglycans. *J Cell Sci* 113(Pt 2): 193–205.
11. Sarrazin S, Lamanna WC, Esko JD (2011) Heparan sulfate proteoglycans. *Cold Spring Harb Perspect Biol* 3(7):pii: a004952.
12. Fuster MM, Esko JD (2005) The sweet and sour of cancer: Glycans as novel therapeutic targets. *Nat Rev Cancer* 5(7):526–542.
13. Wuyts W, et al. (1998) Mutations in the EXT1 and EXT2 genes in hereditary multiple exostoses. *Am J Hum Genet* 62(2):346–354.
14. Yogalingam G, et al. (2004) Identification and molecular characterization of alpha-L-iduronidase mutations present in mucopolysaccharidosis type I patients undergoing enzyme replacement therapy. *Hum Mutat* 24(3):199–207.
15. Baasanjav S, et al. (2011) Faulty initiation of proteoglycan synthesis causes cardiac and joint defects. *Am J Hum Genet* 89(1):15–27.
16. Nakajima M, et al. (2013) Mutations in B3GALT6, which encodes a glycosaminoglycan linker region enzyme, cause a spectrum of skeletal and connective tissue disorders. *Am J Hum Genet* 92(6):927–934.
17. Bui C, et al. (2014) XYLT1 mutations in Desbuquois dysplasia type 2. *Am J Hum Genet* 94(3):405–414.
18. Tagliabracci VS, Pinna LA, Dixon JE (2013) Secreted protein kinases. *Trends Biochem Sci* 38(3):121–130.
19. Xiao J, Tagliabracci VS, Wen J, Kim SA, Dixon JE (2013) Crystal structure of the Golgi casein kinase. *Proc Natl Acad Sci USA* 110(26):10574–10579.
20. Moses J, Oldberg A, Cheng F, Fransson LA (1997) Biosynthesis of the proteoglycan decorin—transient 2-phosphorylation of xylose during formation of the trisaccharide linkage region. *Eur J Biochem* 248(2):521–526.
21. von Marschall Z, Fisher LW (2010) Decorin is processed by three isoforms of bone morphogenetic protein-1 (BMP1). *Biochem Biophys Res Commun* 391(3):1374–1378.
22. Couchman JR, Tapanadechopone P (2001) Detection of proteoglycan core proteins with glycosaminoglycan lyases and antibodies. *Methods Mol Biol* 171:329–333.
23. Hase S, et al. (1988) A new trisaccharide sugar chain linked to a serine residue in bovine blood coagulation factors VII and IX. *J Biochem* 104(6):867–868.
24. Moloney DJ, et al. (2000) Mammalian Notch1 is modified with two unusual forms of O-linked glycosylation found on epidermal growth factor-like modules. *J Biol Chem* 275(13):9604–9611.
25. Whitworth GE, Zandberg WF, Clark T, Vocadlo DJ (2010) Mammalian Notch is modified by D-Xyl-alpha1-3-D-Xyl-alpha1-3-D-Glc-beta1-O-Ser: Implementation of a method to study O-glucosylation. *Glycobiology* 20(3):287–299.
26. David G, Bai XM, Van der Schueren B, Cassiman JJ, Van den Berghe H (1992) Developmental changes in heparan sulfate expression: In situ detection with mAbs. *J Cell Biol* 119(4):961–975.
27. Morelle W, Faid V, Chirat F, Michalski JC (2009) Analysis of N- and O-linked glycans from glycoproteins using MALDI-TOF mass spectrometry. *Methods Mol Biol* 534:5–21.
28. Hellerqvist CG (1990) Linkage analysis using Lindberg method. *Methods Enzymol* 193: 554–573.
29. Rillahan CD, et al. (2012) Global metabolic inhibitors of sialyl- and fucosyltransferases remodel the glycome. *Nat Chem Biol* 8(7):661–668.
30. Bai X, et al. (2001) Biosynthesis of the linkage region of glycosaminoglycans: cloning and activity of galactosyltransferase II, the sixth member of the beta 1,3-galactosyltransferase family (beta 3GalT6). *J Biol Chem* 276(51):48189–48195.
31. Tone Y, et al. (2008) 2-o-phosphorylation of xylose and 6-o-sulfation of galactose in the protein linkage region of glycosaminoglycans influence the glucuronyltransferase-I activity involved in the linkage region synthesis. *J Biol Chem* 283(24):16801–16807.
32. Nadanaka S, et al. (2013) EXTL2, a member of the EXT family of tumor suppressors, controls glycosaminoglycan biosynthesis in a xylose kinase-dependent manner. *J Biol Chem* 288(13):9321–9333.
33. Yamada S, et al. (2002) Determination of the glycosaminoglycan-protein linkage region oligosaccharide structures of proteoglycans from Drosophila melanogaster and Caenorhabditis elegans. *J Biol Chem* 277(35):31877–31886.
34. Ueno M, Yamada S, Zako M, Bernfield M, Sugahara K (2001) Structural characterization of heparan sulfate and chondroitin sulfate of syndecan-1 purified from normal murine mammary gland epithelial cells. Common phosphorylation of xylose and differential sulfation of galactose in the protein linkage region tetrasaccharide sequence. *J Biol Chem* 276(31):29134–29140.
35. Koike T, Izumikawa T, Sato B, Kitagawa H (2014) Identification of phosphatase that dephosphorylates xylose in the glycosaminoglycan-protein linkage region of proteoglycans. *J Biol Chem* 289(10):6695–6708.
36. Quentin E, Gladen A, Rodén L, Kresse H (1990) A genetic defect in the biosynthesis of dermatan sulfate proteoglycan: Galactosyltransferase I deficiency in fibroblasts from a patient with a progeroid syndrome. *Proc Natl Acad Sci USA* 87(4):1342–1346.
37. Schreml J, et al. (2014) The missing "link": An autosomal recessive short stature syndrome caused by a hypofunctional XYLT1 mutation. *Hum Genet* 133(1):29–39.
38. Malfait F, et al. (2013) Defective initiation of glycosaminoglycan synthesis due to B3GALT6 mutations causes a pleiotropic Ehlers-Danlos-syndrome-like connective tissue disorder. *Am J Hum Genet* 92(6):935–945.
39. Lee JE, Fusco ML, Saphire EO (2009) An efficient platform for screening expression and crystallization of glycoproteins produced in human cells. *Nat Protoc* 4(4):592–604.
40. Reed CC, Iozzo RV (2002) The role of decorin in collagen fibrillogenesis and skin homeostasis. *Glycoconj J* 19(4-5):249–255.
41. Tkachenko E, Rhodes JM, Simons M (2005) Syndecans: New kids on the signaling block. *Circ Res* 96(5):488–500.
42. Svensson G, Awad W, Håkansson M, Mani K, Logan DT (2012) Crystal structure of N-glycosylated human glypican-1 core protein: structure of two loops evolutionarily conserved in vertebrate glypican-1. *J Biol Chem* 287(17):14040–14051.
43. Boch J, et al. (2009) Breaking the code of DNA binding specificity of TAL-type III effectors. *Science* 326(5959):1509–1512.
44. Cermak T, et al. (2011) Efficient design and assembly of custom TALEN and other TAL effector-based constructs for DNA targeting. *Nucleic Acids Res* 39(12):e82.
45. Qiu P, et al. (2004) Mutation detection using Surveyor nuclease. *Biotechniques* 36(4): 702–707.
46. Khatua B, Van Vleet J, Choudhury BP, Chaudhry R, Mandal C (2014) Sialylation of outer membrane porin protein D: A mechanistic basis of antibiotic uptake in Pseudomonas aeruginosa. *Mol Cell Proteomics* 13(6):1412–1428.
47. Ciucanu I, Kerek F (1984) A simple and rapid method for the permethylation of carbohydrates. *Carbohydr Res* 131(2):209–217.
48. Damerell D, et al. (2012) The GlycanBuilder and GlycoWorkbench glycoinformatics tools: Updates and new developments. *Biol Chem* 393(11):1357–1362.